GENIORS

Research and Innovation Action (RIA)

This project has received funding from the European Union's Horizon 2020 research and innovation programme under grant agreement No 755171.

Start date : 2017-06-01 Duration : 48 Months
http://geniors.eu/

Report on the speciation and extraction of key fission products

Authors : Mr. Andreas GEIST (KIT), Andreas Geist (KIT), Giuseppe Modolo, Andreas Wilden (JUELICH), Thomas Dumas (CEA)

GENIORS - Contract Number: 755171

Project officer: Roger Garbil

Document title	Report on the speciation and extraction of key fission products
Author(s)	Mr. Andreas GEIST, Andreas Geist (KIT), Giuseppe Modolo, Andreas Wilden (JUELICH), Thomas Dumas (CEA)
Number of pages	27
Document type	Deliverable
Work Package	WP1
Document number	D1.1
Issued by	KIT
Date of completion	2020-01-07 15:23:48
Dissemination level	Public

Summary

Deliverable D1.1, Report on the speciation and extraction of key fission products, compiles distribution data for the extraction of Sr(II) and Fe(III) into TODGA solvents, and Ru(III) speciation and extraction data.

Approval

Date	By
2020-01-07 16:21:31	Mr. Modolo GIUSEPPE (FZJ)
2020-01-08 08:02:21	Mr. Andreas GEIST (KIT)
2020-04-22 09:13:28	Mr. Stéphane BOURG (CEA)

CONTENT

This project has received funding from the EURATOM research and training programme 2014–2018 under grant agreement No 730227

This project has received funding from the EURATOM research and training programme 2014–2018 under grant agreement No 730227

EXECUTIVE SUMMARY

Deliverable D1.1, Report on the speciation and extraction of key fission products, compiles distribution data for the extraction of Sr(II) and Fe(III) into TODGA solvents, and Ru(III) speciation and extraction data.

This project has received funding from the EURATOM research and training programme 2014–2018 under grant agreement No 730227

Sr(II) EXTRACTION INTO TODGA

N,N,N',N'-tetra-n-octyl diglycolamide (TODGA)[1-4] is used in numerous processes developed and tested in Europe for co-extracting actinide and lanthanide ions.[5] To better understand and quantify the (unwanted) co-extraction of Sr(II), distribution ratios for the extraction of Sr(II) into various TODGA based solvents were determined.

TPH/OCTANOL DILUENT

The co-extraction of Sr(II) is an issue with TODGA based solvents. Some data are available in the literature, however none for a solvent composed of TODGA + 5% octanol in TPH. Sr(II) distribution data for a solvent without and with 0.5 mol/L TBP as modifier are available.[2]

Distribution data were determined for the extraction of Sr(II) from HNO_3 into a solvent containing TODGA + 5% octanol in TPH as a function of contact time and HNO_3 and TODGA concentrations.

EXPERIMENTAL

Organic phases were 0.05–0.3 mol/L TODGA + 5 vol.-% 1-octanol in TPH or 0.2 mol/L TODGA + 0.5 mol/L TBP in TPH. Aqueous phases were 10^{-4} mol/L $Sr(NO_3)_2$ in 0.1–5 mol/L HNO_3 or 2.9 mol/L NH_4NO_3 (pH 2). Each 500 µL organic and aqueous phases were contacted in 2 mL screw-cap glass vials on a temperature-controlled shaker (t = 30 min, f = 2500/min, T = 20 °C). As revealed by an initial test, equilibrium was attained within several minutes. After centrifugation, aqueous aliquots were diluted with 0.1 mol/L HNO_3 suprapure, organic aliquots were stripped into 0.1 mol/L HNO_3 suprapure (A/O = 10). Sr concentrations were determined by ICP-MS.

RESULTS

Figure 1 shows Sr(II) distribution data for varied initial HNO_3 and TODGA concentrations. The distribution data show a maximum at an initial HNO_3 concentration of ≈ 3 mol/L. For a TODGA concentration of 0.2 mol/L and HNO_3 concentrations greater than 0.9 mol/L, Sr(II) distribution ratios are greater than 1. This explains the significant Sr(II) recycling observed in process tests, with $D_{Sr(II)} > 1$ in the extraction section (operating at ≈ 3 mol/L HNO_3) and $D_{Sr(II)} < 1$ in the scrubbing section (operating at ≈ 0.5 mol/L HNO_3). Sr(II) distribution ratios are significantly lower for the TPB modifier (small blue triangles) at lower HNO_3 concentrations; no difference is found beyond 1 mol/L HNO_3. The difference to the data from reference[2] (blue asterisks) is explained by partial loading of the solvent in the former case (with several metal ions at 10 mmol/L each present in the aqueous phase).

This project has received funding from the EURATOM research and training programme 2014–2018 under grant agreement No 730227

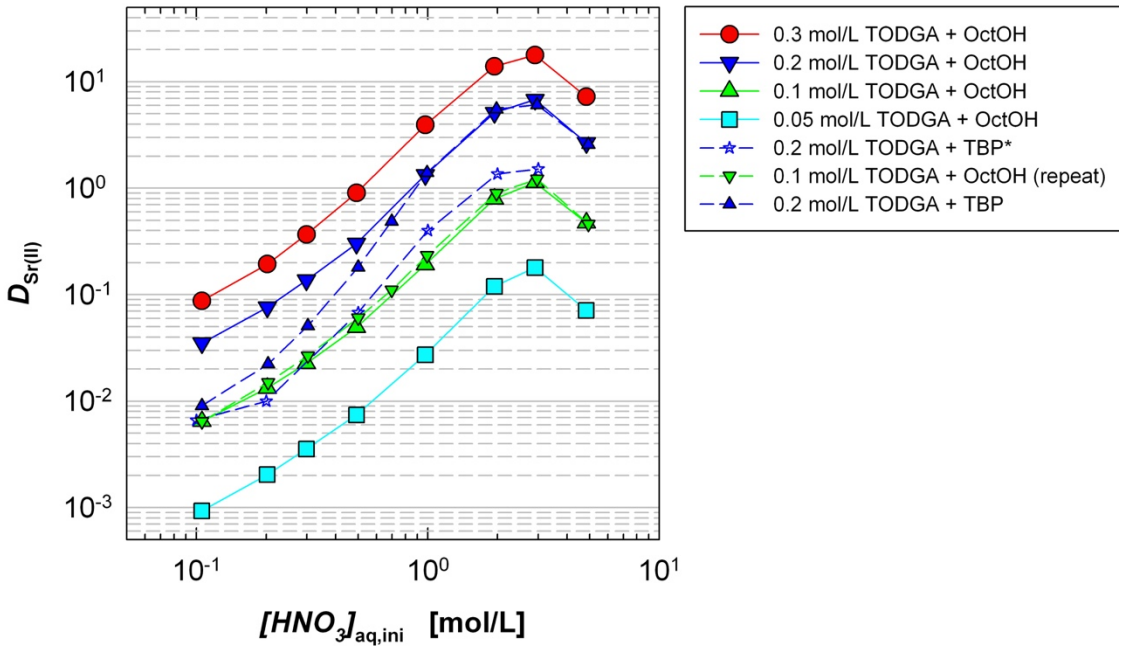

Figure 1. Extraction of Sr(II) from HNO_3 into TODGA solvents as a function of initial HNO_3 concentration. Organic phase, TODGA + 5% octanol in TPH. Aqueous phase, 10^{-4} mol/L $Sr(NO_3)_2$ in HNO_3. *A/O* = 1, *T* = 20 °C. (*data from ref.[2] 0.2 mol/L TODGA + 0.5 mol/L TBP in TPH, 0.01 mol/L Sr(II), *T* = 22 °C).

A simple slope analysis of the distribution data was performed. This is valid for lower HNO_3 concentrations, 0.1–0.5 mol/L, where $[HNO_3]_{aq,eq} \approx [HNO_3]_{aq,ini}$ and $[TODGA]_{free} \approx$ constant. Slopes of 2.5–2.7 (Figure 2) indicate the presence of both 1:2 and 1:3 complexes.

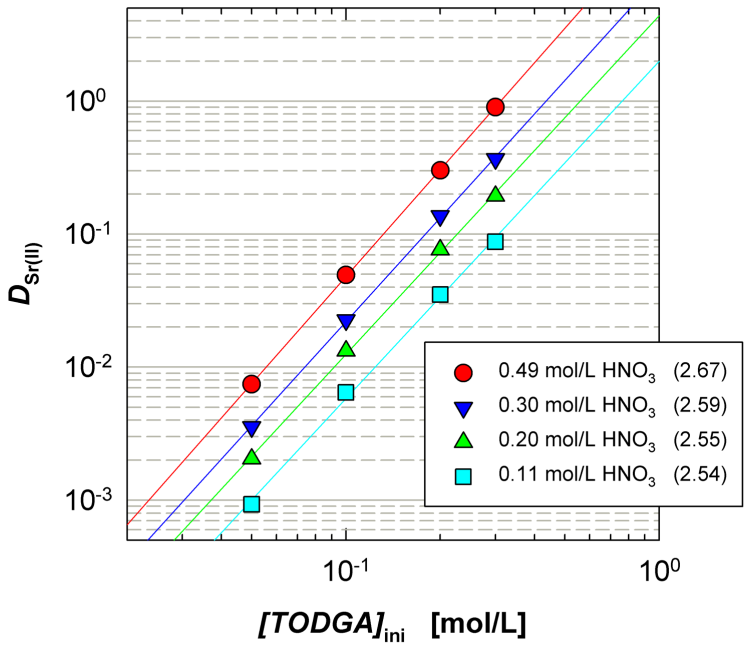

Figure 2. Extraction of Sr(II) from HNO_3 into TODGA solvents as a function of initial TODGA concentration. Organic phase, TODGA + 5% octanol in TPH. Aqueous phase, 10^{-4} mol/L $Sr(NO_3)_2$ in HNO_3. *A/O* = 1, *T* =20 °C.

This project has received funding from the EURATOM research and training programme 2014–2018 under grant agreement No 730227

Further distribution data as a function TODGA concentration were determined. To preclude HNO_3 extraction, the aqueous phase was a solution of NH_4NO_3. In agreement with results presented in Figure 2 (with HNO_3 aqueous phases), the slope is 2.7, see Figure 3.

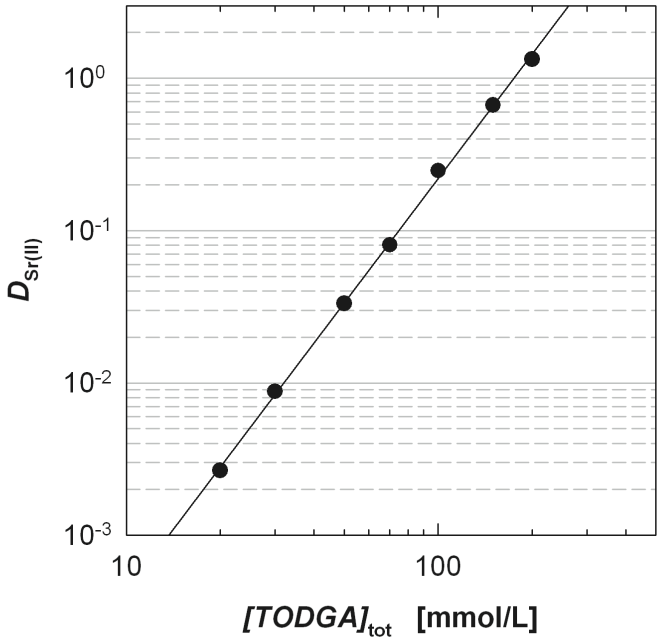

Figure 3. Extraction of Sr(II) from HNO_3 into TODGA as a function of initial TODGA concentration. Organic phase, TODGA + 5% octanol in TPH. Aqueous phase, 10^{-4} mol/L $Sr(NO_3)_2$ in 2.9 mol/L NH_4NO_3 (pH 2). *A/O* = 1, *T* =20 °C.

CONCLUSION

In a solvent extraction process using the commonly applied TODGA solvent (0.2 mol/L TODGA + 5 vol.% 1-octanol in TPH), Sr(II) is extracted in the extraction section ($D_{Sr(II)} \approx 7$) and scrubbed in the scrubbing section ($D_{Sr(II)} \approx 0.3$), see Figure 1. This leads to significant Sr(II) accumulation in the extraction section. Reducing the TODGA concentration to 0.1 mol/L would mitigate this behaviour.

AROMATIC DILUENTS

TODGA solvents studied so far require the addition of a phase modified to suppress third phase formation upon loading with metal nitrates.[4] A simpler solvent composition is desirable, ideally one extractant in one diluent. This is achieved using aromatic diluents:[6] 1,4-diisopropyl benzene (DIPB) was tested as an alternative to the TPH/1-octanol diluent. Sr(II) distribution ratios were determined and compared to the TODGA-1-octanol-TPH solvent.

This project has received funding from the EURATOM research and training programme 2014–2018 under grant agreement No 730227

EXPERIMENTAL

Organic phases were TODGA in DIPB or TPH + 5 vol.% 1-octanol. Aqueous phases were either 3×10^{-4} mol/L Sr(II) in HNO_3 or 10^{-4} – 1 mol/L Sr(II) + 1 kBq ^{241}Am(III) + ^{154}Eu(III) in 1 mol/L HNO_3. Further proceeding was as described above. ^{241}Am(III) and ^{154}Eu(III) were determined by gamma counting.

RESULTS

Figure 4 shows Sr(II) distribution data for varied initial HNO_3 and TODGA concentrations. Sr(II) distribution ratios show a maximum at an initial HNO_3 concentration of ≈ 3 mol/L, as observed with the 1-octanol/TPH diluent (Figure 1). For a TODGA concentration of 0.5 mol/L and HNO_3 concentrations greater than 0.7 mol/L, Sr(II) distribution ratios are greater than 1.

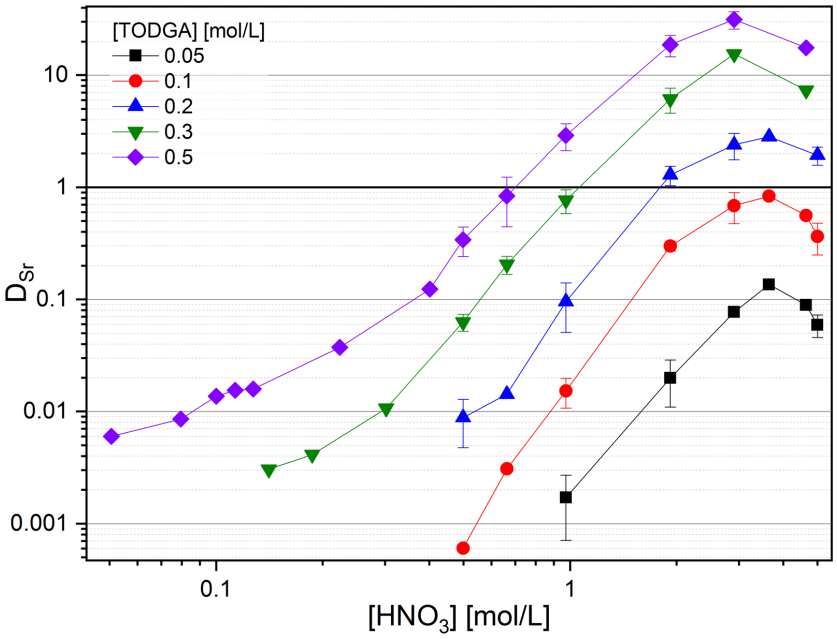

Figure 4. Sr(II) extraction into TODGA in DIPB, distribution ratios as a function of initial HNO_3 concentration. Organic phase, TODGA in DIPB. Aqueous phase, 3×10^{-4} mol/L Sr(II) in HNO_3. *A/O* = 1, *T* =20 °C.

A simple slope analysis of the distribution data was performed, Figure 5. The slope of lg $D_{Sr(II)}$ vs. lg [*TODGA*] decreases from 4 (for 0.5 mol/L HNO_3) to ≈ 3 (for 1–2 mol/L HNO_3). The value of 2.3 (4.6 mol/L HNO_3) must not be stressed since the prerequisites for applying slope analysis are definitely not met for such conditions.

Slopes significantly greater than three have also been observed for the extraction of Am(III) into TODGA in DIPB.[6] This deviation from the spectroscopically verified formation of 1:3

This project has received funding from the EURATOM research and training programme 2014–2018 under grant agreement No 730227

complexes may be explained by outer sphere complexation by a fourth TODGA molecule. A similar mechanism may be assumed for the extraction of Sr(II) at lower HNO_3 concentrations.

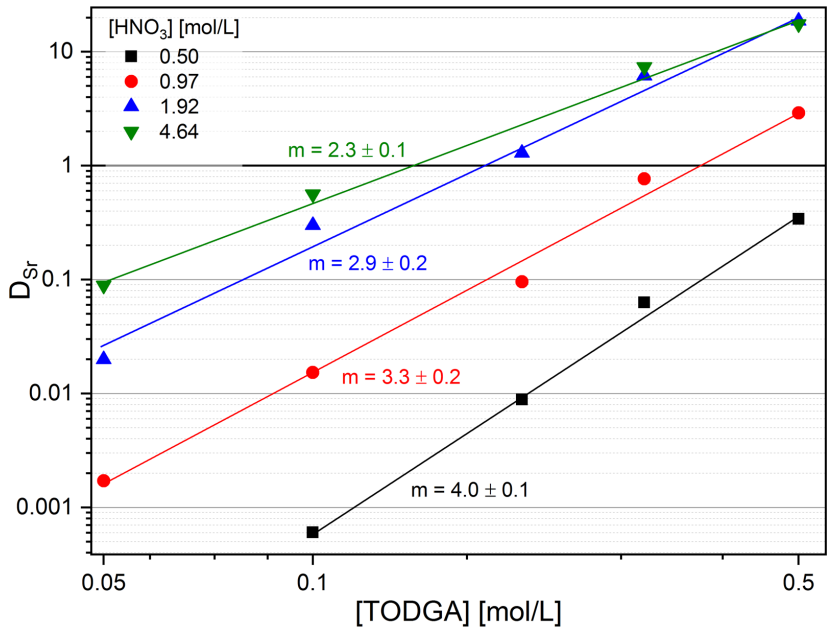

Figure 5. Sr(II) extraction into TODGA in DIPB, distribution ratios as a function of total TODGA concentration. Organic phase, TODGA in DIPB. Aqueous phase, 3×10^{-4} mol/L Sr(II) in HNO_3. *A/O* = 1, *T* =20 °C.

Figure 6 shows Sr(II) distribution ratios (top) and the organic equilibrium Sr(II) concentration as a function of the initial aqueous Sr(II) concentration (bottom). The effect of Sr(II) loading on Am(III) and Eu(III) extraction is shown in Figure 7.

Sr(II) is less extracted with the DIPB-based solvent compared to the TPH/octanol based solvent; distribution ratios for non-loading conditions are lower by approximately one order of magnitude. However, at an initial Sr(II) concentration of 1 mol/L almost the same distribution ratios are found, $D_{Sr(II)} \approx 0.02$, with organic phase Sr(II) concentrations of ≈ 0.02 mol/L.

For both solvents, Am(III) and Eu(III) distribution ratios remain constant up to initial Sr(II) concentrations lower than 0.025 mol/L. With the TPH/octanol diluent, Am(III) and Eu(III) distribution ratios slightly decrease beyond 0.025 mol/L Sr(II) due to partial loading of the solvent. With DIPB, distribution ratios slightly increase. This is due to the increase in nitrate concentration upon addition of $Sr(NO_3)_2$. The separation factor $SF_{Eu/Am}$ remains constant and independent of the used solvent or initial Sr(II) concentration.

This project has received funding from the EURATOM research and training programme 2014–2018 under grant agreement No 730227

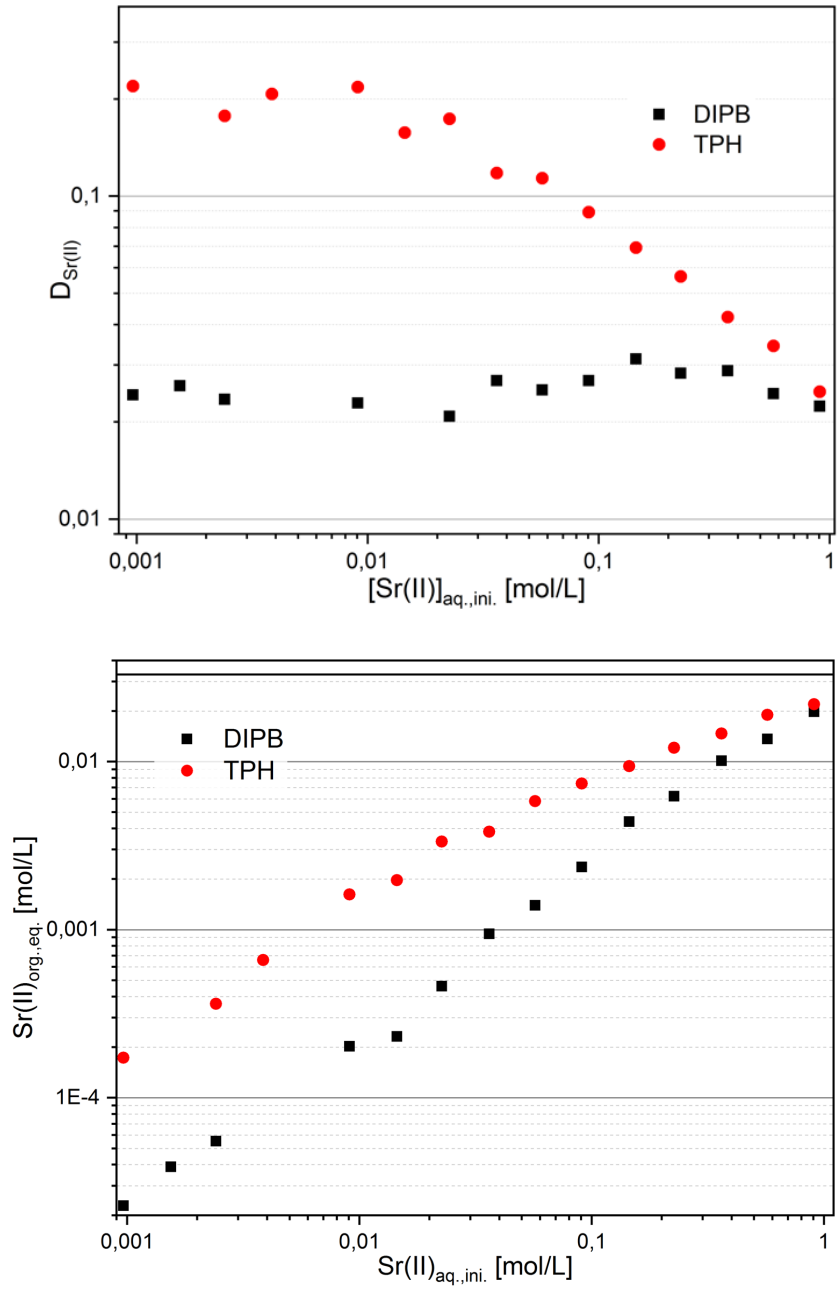

Figure 6. Sr(II) extraction into TODGA solvents, Sr(II) distribution ratios (top) and organic equilibrium Sr(II) concentration (bottom) as a function of initial aqueous Sr(II) concentration. Organic phase, 0.1 mol/L TODGA in DIPB or TPH + 5 vol.% 1-octanol. Aqueous phase, 10^{-4} – 1 mol/L Sr(II) and 1 kBq ^{241}Am(III) and ^{154}Eu(III) in 1 mol/L HNO_3. *A/O* = 1, *T* =20 °C.

This project has received funding from the EURATOM research and training programme 2014–2018 under grant agreement No 730227

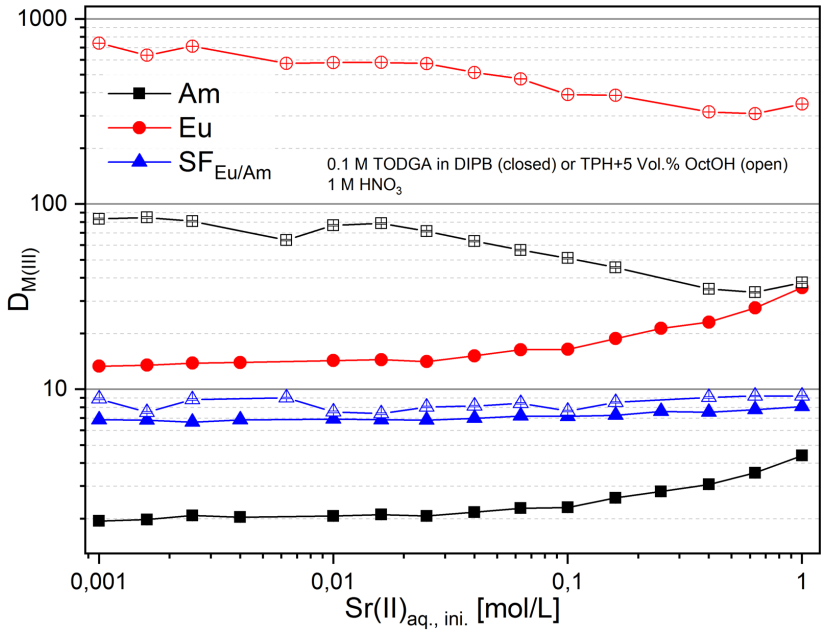

Figure 7. Sr(II) extraction into TODGA solvents, Am(III) and Eu(III) distribution ratios under Sr(II) loading. Experimental conditions, see Figure 6.

CONCLUSION

As with the 1-octanol/TPH diluent, accumulation of Sr(II) is expected in a process using the TODGA-DIPB diluent if the TODGA concentration is greater than 0.1 mol/L.

This project has received funding from the EURATOM research and training programme 2014–2018 under grant agreement No 730227

BEHAVIOUR OF Fe(III) IN TODGA SYSTEMS

The extraction of ^{55}Fe(III) into TODGA was studied as iron is discussed as one of the possibly problematic fission and corrosion products in the i-SANEX[7] and AMSEL[8] processes.

Therefore, the extraction of Fe(III) was studied as a function of nitric acid and TODGA concentrations. Figure 8 shows that low distribution ratios were observed under all conditions. Nevertheless, a slight increase in distribution ratios is observed for very low and for higher HNO_3 concentrations.

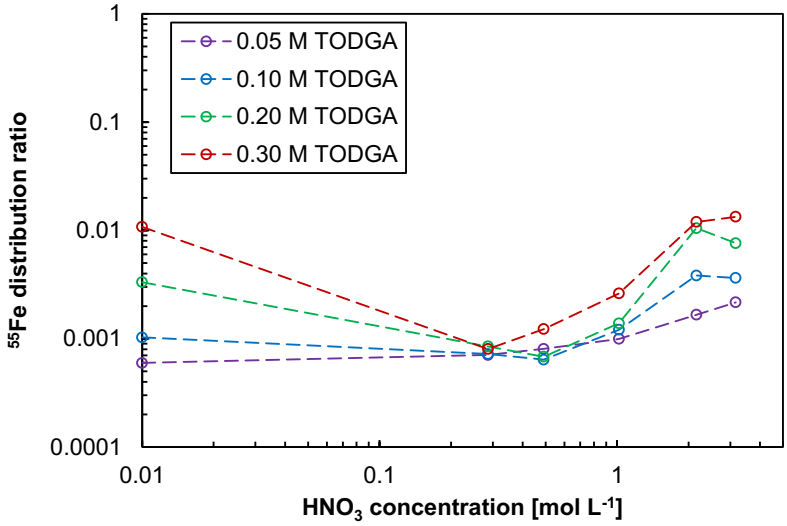

Figure 8. ^{55}Fe(III) distribution ratios as a function of the HNO_3 concentration for different concentrations of TODGA. Organic phase, TODGA + 5 vol.-% 1-octanol in TPH; Aqueous phase, Ln(III) (10^{-4} mol/L each) + ^{55}Fe(III) tracer in HNO_3.

This project has received funding from the EURATOM research and training programme 2014–2018 under grant agreement No 730227

EXTRACTION AND SPECIATION OF Ru(III)

INTRODUCTION

In order to recover material from spent nuclear fuel while minimising the volume of high-level nuclear waste, separation based on solvent extraction process are used. Currently, the PUREX process, using 30% (1.1 mol/L) tributyl phosphate (TBP) in TPH is industrialized in France. The TBP solvent also extracts small amounts of certain fission products that need to be removed in order to recover uranium and plutonium with the required purity. One extracted fission product is ruthenium.[9]

Distribution ratios of ruthenium vary as a function of the nitric acid concentration and the ruthenium species. In nitric acid and TBP solvents, ruthenium has been investigated since the 1950s. Former research identified diverse octahedral ruthenium nitrosyl complexes in nitric acid solutions. Siszek *et al.* defined a general formula (1) for ruthenium nitrosyl complexes in nitric acid solution:[9-12]

$$[Ru(NO)(NO_2)_x(NO_3)_y(OH)_z(H_2O)_{5-x-y-z}]^{3-x-y-z} \quad (1)$$

Recent studies by Lefebvre *et al.*[9, 11, 13] used a complementary approach of EXAFS and FTIR spectroscopy to determine the predominant $[Ru(NO)(NO_3)_3(H_2O)_2]^0$ structure in TBP solvent extraction from 4 mol/L nitric acid. In contrast, extraction from 1 mol/L nitric acid results in the predominant formation of hydrolysed $[Ru(NO)(NO_3)_2(OH)(H_2O)_2]^0$ complexes. Under both extraction conditions, TBP only interacts in the second coordination sphere of the ruthenium complexes.

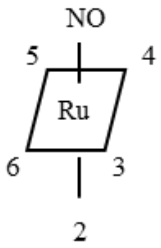

Figure 9. Illustration of pseudo-octahedral ruthenium nitrosyl complex in which all edges represent a ligand position.

This report summarises recent investigations on ruthenium speciation in extraction and stripping experiments. TBP is used as a reference solvent extraction system; the study is extended to other extracting system such as monoamides and TODGA. Nitrous acid has an important impact of on ruthenium(III) speciation in 1 mol/L and 5 mol/L nitric acid, impacting

This project has received funding from the EURATOM research and training programme 2014–2018 under grant agreement No 730227

both distribution ratios and speciation in the organic phase. Distribution ratios were quantified by ICP-AES as a function of the nitric acid concentration and with varying initial nitrous acid concentrations and in various extraction systems. For extractions with particularly high distribution ratios, the organic phases were specified by Electro Spray Ionisation Mass Spectrometry (ESI-MS), Fourier Transform Infra-Red (FTIR) and sometimes Extended X-ray Absorption Fine Structure (EXAFS). The aqueous solutions were characterised before and after extraction using RAMAN spectroscopy. Experimental details on sample preparation and analysis are found in reference.[14]

SOLVENT EXTRACTION FROM NITRIC ACID SOLUTION

GENERAL ASPECT OF RUTHENIUM SOLVENT EXTRACTION AND ANALYTICAL METHODS

As mentioned, the numerous nitrosyl (RuNO) complexes appears in nitric acid in form of a pseudo-octahedral geometry. In this complex the nitrosyl-Ru bond is shorter than the other five other bonds with nitrate, hydroxo, nitrite or water ligand. In the organic phase, Fletcher et al.[15] as well as Lefebvre et al.[9, 11, 13] excluded the presence of TBP in the inner coordination sphere of RuNO complexes and proposed (respectively from sequential solvent extraction studies or FTIR/EXFAS measurements) that TBP interacts via hydrogen bonds to water and hydroxyl ligands from RuNO complexes. Nevertheless, this ruthenium polydispersity in nitric acid solution influences its behaviour in solvent extraction and complicates its understanding. Moreover, the slow ligand exchange kinetics in ruthenium complexes make experimental reproducibility challenging, requiring long equilibration times to attain chemical equilibrium.

As an example of polydispersity, hydroxide ligands (not stable in 4 mol/L nitric acid and when extracted from 4 mol/L nitric acid into TBP[9-10, 12]) coordinate to ruthenium for nitric acid concentrations < 2 mol/L. Under such conditions, ruthenium nitrosyl complexes contain a hydroxyl group in the axial position (2).[9] Hence, the nitric acid concentration in the initial aqueous phase defines the commonness of single ruthenium nitrosyl complexes in TBP solvent extraction phases.[10, 13, 16]

$$[RuNO(NO_3^-)_x(OH^-)_{ax,z}(H_2O)_{4-x}(H_2O)_{ax(1-z)}]^{(3-x-z)+} \quad (2)$$

Experimentally, these complexes are distinguished[13, 16] by the FTIR nitrosyl vibrations at ν= 1850–1950 cm^{-1}. These vibrations mainly depend on the nature of the ligand in axial position. Besides this nitrosyl ligand vibration, ruthenium complexes can be studied in the organic phase regarding nitrate vibrations. Asymmetric and symmetric nitrogen-oxygen bond stretching of complexing nitrates are recorded in the range of 1531–1481 cm^{-1} and 1296–

This project has received funding from the EURATOM research and training programme 2014–2018 under grant agreement No 730227

1253 cm^{-1}, respectively.[9, 11, 13, 17-18] Furthermore, information on the extracting agents' functions are available from the corresponding stretching frequencies.

SOLVENT EXTRACTION PROPERTIES AND SPECTROSCOPIC INVESTIGATIONS

In order to assign the ruthenium speciation in alternative solvent extraction system such as monoamides, a FTIR study similar to the one proposed by Lefebvre et al. was performed using a monoamide (MOEHA is used as a surrogate of DEHiBA for its better extraction properties, resulting in stronger spectroscopic signals) and TODGA ligands. As complementary experiment, the ruthenium extraction properties measured for different extracting molecules is presented in Figure 10. The resulting D_{Ru} values are plotted as a function of the initial nitric acid concentration (left) and as a function of the water extraction properties (b). The three solvent exhibit a bell-shaped curve typical in case of extraction of metal-nitrate neutral complexes by the three molecules. Indeed, the previous speciation studies confirmed that the main ruthenium species extracted from 3 mol/L acidic feeds are trinitrate ruthenium nitrosyl complexes. But some differences must be emphasised to specify each solvent's properties. The three bell-shaped curves are neither symmetrical nor centred at the same acidity showing different competitive extraction equilibrium toward nitric acid extraction and as already mentioned a different complex extraction at lower acidity. Further speciation analysis of ruthenium species was conducted to assign the different solvent behaviour.

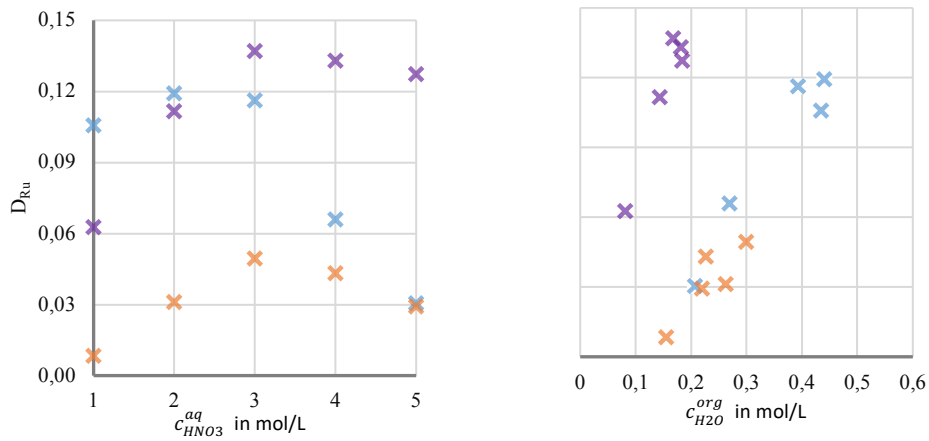

Figure 10. Ruthenium distribution ratio as a function of (left) aqueous phase nitric acid equilibrium concentration and (right) organic phase water equilibrium concentration. Blue, TBP; purple, TODGA; orange, MOEHA.

Figure 11 displays the corresponding MOEHA and TODGA FTIR spectra (TBU, tetrabutyl urea displayed for comparison) obtained after solvent extraction from a 4 mol/L nitric acid solution is compared to TBP (blue) organic phase (identical extraction conditions). For comparison, each spectrum is subtracted with the corresponding pre-equilibrated solvent before

This project has received funding from the EURATOM research and training programme 2014–2018 under grant agreement No 730227

ruthenium extraction and normalised to the ruthenium concentration in the organic phase. For the three solvent extraction systems, the ruthenium nitrosyl complexes FTIR signal (i.e. nitrosyl vibrations at ν = 1850–1950 cm^{-1}, and complexing nitrates at 1531–1481 cm^{-1} and 1296–1253 cm^{-1}) are identical to those measured in the initial aqueous phase. At 4 mol/L nitric acid, the complexing nitrates are maintained as the predominant ligand in the equatorial plane. Only water molecules (no hydroxyl groups) are detected in the ruthenium axial position whatever the extracting molecule. As with the TBP system, ruthenium extraction from 4 mol/L nitric acid proceeds via weak outer sphere interactions, probably involving H-bonded extractant molecules. This is confirmed by the absence of any deformation of the monoamide (or carbamide) carbonyl function at 1600 cm^{-1}, in contrast to uranium or plutonium extraction.[19]

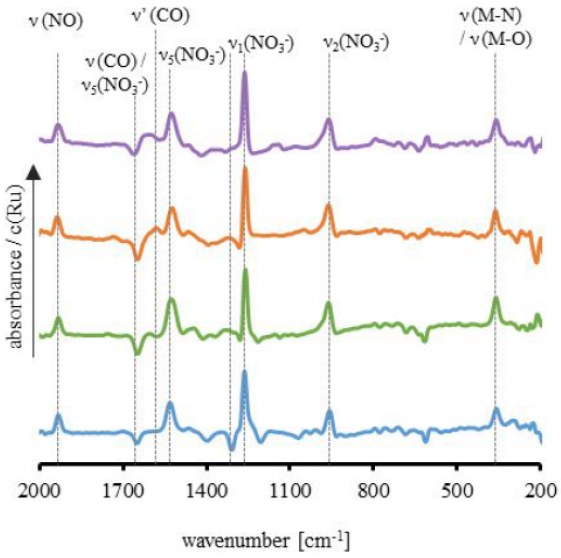

Figure 11. Differential FTIR spectra of (blue) TBP, (green) TBU, (orange) MOEHA and (purple) TODGA showing ruthenium complexes' FTIR signals after nitric acid pre-contact spectra subtraction. Vibrations of interest are marked by dashed lines and assigned to the corresponding ligands/functions.

Results from X-ray absorption spectroscopy confirm this ruthenium speciation. The EXAFS spectra presented Figure 12 again indicate that the composition of the first coordination sphere is invariable with the extracting agent. The spectra of the pseudo radial distribution functions (k^3 weighted EXAFS oscillations) show three main peaks or coordination shells similar to those observed by Lefebvre et al.[9, 11, 13] As proven previously in the TBP system, the first shell accounts for five oxygen atoms from water and nitrate ligands and one nitrogen from the nitrosyl group. The second shell is more complex; signals from the nitrosyl O atom (short) and from the nitrate N atoms (long) are superimposed with strong multiple scattering from the linear nitrosyl ligand. However, regardless of which ligands they represent, the pseudo-radial distribution functions are similar to each other. Consistently with the FTIR analysis, this

This project has received funding from the EURATOM research and training programme 2014–2018 under grant agreement No 730227

evidences that the extracting agent does have an effect on the ruthenium first coordination sphere. No extracting function enter the ruthenium coordination sphere and extraction is performed through weak hydrogen bonds to coordinating water molecules.

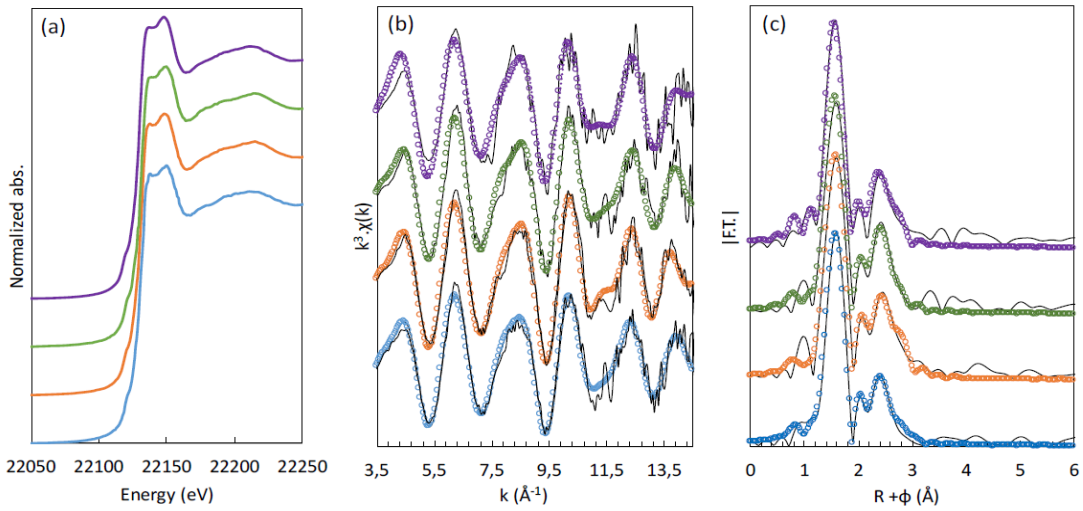

Figure 12. (a) normalised Ru K edges, (b) k^3-weighed EXAFS spectra and (c) corresponding Fourier transformation for Ru extractions with (blue) TBP, (green) TBU, (orange) MOEHA and (purple) TODGA.

For lower acid conditions (1 mol/L HNO_3), the monoamide system contrast with the TBP one. No ruthenium complexes with hydroxide group was detected in organic phase during 1 mol/L nitric acid experiment (EXAFS and FTIR not shown here). It agrees with bell shaped distribution ratio curve, in contrast with that for TBP (Figure 10). While for the TBP system, the maximum extraction is observed for 2 mol/L nitric acid in the aqueous phase, the amide-based extraction systems reach a maximum for 3–4 mol/L with very low distribution ratio for lower nitric acid conditions. This is because the hydrolysed ruthenium complexes identified with TBP is not or only poorly extracted by monoamides system. The TODGA system is intermediate with less ruthenium complexes with hydroxide group observed compared to TBP.

CONCLUDING REMARKS ON RUTHENIUM SOLVENT EXTRACTION

The results have shown that none of the studied extractants interacts with ruthenium directly, after extractions from 4 mol/L nitric acid. The same analysis performed at 3 mol/L nitric acid provide identical conclusions. The absence of extractant-ruthenium interaction was proven by the absence of a carbonyl/phosphoryl and nitrosyl shifts in the FTIR spectra, and by EXAFS spectroscopy. Furthermore, all spectra indicate a similar inner sphere coordination of ruthenium in 4 mol/L nitric acid and in all corresponding organic solvents after extraction. Differences in the ruthenium distribution ratios for extraction from 4 mol/L nitric acid are driven by outer-sphere interactions in all solvents analysed. TBP, MOEHA and TODGA

This project has received funding from the EURATOM research and training programme 2014–2018 under grant agreement No 730227

predominantly bond to water ligands of ruthenium nitrosyl complexes during extraction. Such hydrogen bond-driven solvent extraction results in a linear relation between ruthenium and water extraction (Figure 10). Consequently, solvents extracting high concentrations of water should favour higher ruthenium co-extraction.

THE IMPACT OF NITRITE ON RUTHENIUM AQUEOUS SPECIATION

In a first instance, solvent extraction studies were not considering the impact of nitrite ligands (z=0). Since our recent speciation study evidenced that ruthenium nitrosyl complexes speciation in aqueous solution can be assigned by the use of RAMAN spectroscopy, we decided to deepen this aspect starting from the ruthenium speciation aqueous solution. In spent nuclear fuel solution and subsequent solvent extraction cycles, nitrites can be formed through chemical reduction or radiolysis of nitric acid and during the fuel dissolution steps. In > 1 mol/L nitric acid solution, nitrites appear in form of nitrous acid, which is very reactive. Either it degrades into water or nitrous gases or is extracted by TBP solvent in which it is more stable, or it reacts with any other component in dissolved spent nuclear fuel, like the fission product ruthenium. In this section, we analyse the impact of dissolved nitrites on ruthenium(III) nitrosyl complexes in 1 mol/L and 5 mol/L nitric acid solution by RAMAN spectroscopy. Solutions of ruthenium(III) nitrosyl nitrate were prepared in 1 mol/L and 5 mol/L nitric acid. All solutions were heated to ≈ 80 °C for 3 h and both 1 mol/L and 5 mol/L nitric acid solutions were separated into five equal volumes. Each of the separated solution was mixed with sodium nitrite in order to obtain concentrations of 0 mol/L, 0.5 mol/L, 1 mol/L, 1.5 mol/L and 2 mol/L. The acidity of each solution was analysed by acid-base titrations, and the nitrite concentrations of each solutions was analysed by the Griess method (see Table 1 for results). The acidities of the samples gradually drop down in presence of nitrites. One explanation is the formation of nitrous acid and its consecutive degradation. However, the acid decrease is not similar in 1 mol/L and 5 mol/L nitric acid solutions. After adding 2 mol/L sodium nitrite, the acidity of the 1 mol/L nitric acid solution decreases by 0.8 mol/L, whereas the acidity in 5 mol/L nitric acid only decreases by 0.3 mol/L. This difference is unexpected, since nitrous acid degradation is expected to be stronger in the 5 mol/L nitric acid solution. Accordingly, another effect must be involved which decreases the acidity in the 1 mol/L nitric acid solutions in presence of enlarged nitrite concentrations. The explanation is likely related to the presence of hydroxide ligands in ruthenium complexes, as already reported for 1 mol/L nitric acid solution. The presence of such hydroxide ligands in ruthenium complexes increases the acidity of the solution, as shown for 1 mol/L nitric acid solution without added sodium nitrite. Whereas a disappearance of hydroxide ligands would decrease the acidity of the solution because of the protonation of hydroxide ligands, as proposed in following equation:

$$[Ru(NO)\dots(OH)] + H_2O \rightleftharpoons [Ru(NO)\dots(H_2O)] + OH^-$$

This project has received funding from the EURATOM research and training programme 2014–2018 under grant agreement No 730227

Both effects together, nitrous acid degradation and hydroxide ligand protonation, likely cause the higher acidity decrease in 1 mol/L. In contrast, the acidity decrease in 5 mol/L nitric acid is only due to nitrous acid degradation, since no hydroxide ligands were reported at such high nitric acid concentrations. The results in Table 1 also show that the measured nitrite concentrations are significantly lower than the initial nitrite concentrations in all samples. Significantly lower nitrite concentrations either come from the nitrous acid degradation degradation or from nitrite immobilization as ligands in the ruthenium coordination sphere, which may be not quantified by the Griess method. The full degradation into nitrous gases is not reasonable, since it would have decreased the acidity more than it was observed. Accordingly, nitrites are likely the coordination sphere of ruthenium complexes.

Table 1. Initial nitric acid and nitrite concentrations vs. measured acidity and nitrite concentrations of a solution of ≈ 0.5 mol/L ruthenium(III) nitrosyl nitrate. All concentrations, mol/L.

Sample #	$[HNO_3]_{ini}$	$[H^+]$	$[NO_2^-]_{ini}$	$[NO_2^-]$ ×1000
1	1	1.32	0	0.40
2	1	1.09	0.5	1.70
3	1	0.66	1	1.67
4	1	0.55	1.5	10.1
5	1	0.49	2	16.8
6	5	4.8	0	0.74
7	5	4.6	0.5	1.32
8	5	4.9	1	1.49
9	5	4.6	1.5	1.51
10	5	4.5	2	1.54

In order to evidence the change in the ruthenium coordination sphere due to nitrites, Raman spectra of the samples were recorded to identify the role of nitrites ligand on the ruthenium speciation (Figure 13).

This project has received funding from the EURATOM research and training programme 2014–2018 under grant agreement No 730227

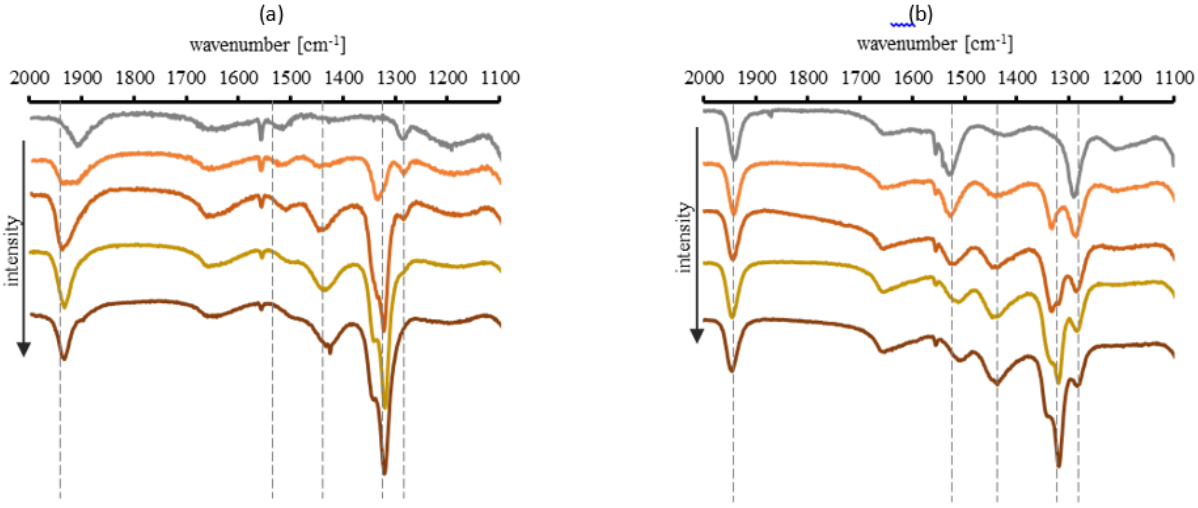

Figure 13. RAMAN spectra of 0.5 mol/L ruthenium nitroysl nitrate in (a) 1 mol/L and (b) 5 mol/L nitric acid solution including sodium nitrite at 0 mol/L (gray), 0.5 mol/L (orange), 1 mol/L (brown), 1.5 mol/L (yellow) and 2 mol/L (dark brown). Spectra are shifted vertically.

The spectra show five vibrations attributed to ruthenium complexes. The vibration ν_{R1} at 1900 cm^{-1} corresponds to the stretching of nitrosyl ligands. In 1 mol/L nitric acid, increasing concentrations of sodium nitrite shift the nitrosyl vibration from 1900 cm^{-1} to 1930 cm^{-1}. Nitrosyl vibration around 1900 cm^{-1} have been assigned to ruthenium complexes with one hydroxide ligand, known as hydrolysed complexes. In contrast, vibrations at 1930 cm^{-1} correspond to non-hydrolysed complexes. Accordingly, the addition of sodium nitrite initialises a transformation from hydrolysed into non-hydrolysed ruthenium complexes in 1 mol/L nitric acid. The disappearance of hydrolysed complexes in the RAMAN spectra agree with the observations of acid-base titrations, showing an increased acidity drop due to the protonation of hydrolysed complexes in 1 mol/L nitric acid. The vibrations ν_{R2} at 1530 cm^{-1} and ν_{R5} at 1280 cm^{-1} correspond to asymmetric and symmetric stretching of nitrate ligands in ruthenium nitrosyl complexes, respectively. These vibrations are stronger in 5 mol/L nitric acid than in 1 mol/L nitric acid since the number of nitrate ligands per ruthenium complex increases with the nitric acid concentration. The addition of sodium nitrite causes a decrease of nitrate ligand vibrations in ν_{R2} and ν_{R5}. The vibrations ν_{R3} at 1420 cm^{-1} and ν_{R4} at 1330 cm^{-1} correspond to asymmetric and symmetric stretching of nitrite ligands, respectively. The intensities of these vibrations increase for higher concentrations of sodium nitrite both in 1 mol/L and in 5 mol/L nitric acid. Increasing intensities show that nitrites enter the coordination sphere of ruthenium nitrosyl complexes. The coordination of nitrites to ruthenium must compete with nitrite degradation in nitric acid. However, in both 1 mol/L and 5 mol/L nitric acid, dissolved nitrites rather coordinate to ruthenium(III) nitrosyl complexes then degrade in form of nitrous acid, as shown by the strong increase of nitrite ligands in the RAMAN spectra. Furthermore, the simultaneous increase of nitrite ligands in ν_{R3} and ν_{R4} and

This project has received funding from the EURATOM research and training programme 2014–2018 under grant agreement No 730227

the decrease of nitrate ligands in ν_{R2} and ν_{R5} indicate a substitution of nitrates by nitrites in the first coordination sphere of ruthenium complexes. The shape of the vibration ν_{R4} changes as a function of the initial sodium nitrite concentration in 1 mol/L and 5mol/L nitric acid solution. For 0.5 mol/L sodium nitrite added to the ruthenium solutions, nitrite ligands in ν_{R4} form a single the peak. For 1 mol/L sodium nitrite added to the ruthenium solutions, an adjacent peak appears in ν_{R4} at slightly lower wavenumbers. It has about the same intensity as the first peak, which was rising for 0.5 mol/L sodium nitrite, in both 1 mol/L and 5 mol/L nitric acid. For 1.5 mol/L sodium nitrite added to the ruthenium solutions, the adjacent peak reaches twice the maximum of the first peak in 1 mol/L nitric acid solution. For 2 mol/L sodium nitrite added to the ruthenium solutions, the vibration vR4 in 1 mol/L nitric acid does not significantly differ from 1.5 mol/L sodium nitrite added. The similarity between 1.5 mol/L and 2 mol/L of added sodium nitrite indicates a saturation of nitrites in the coordination sphere of ruthenium(III) complexes.

The split of ν_{R4} into two adjacent peaks is known for nitrite complexes in RAMAN spectroscopy. In the case of ruthenium (III) nitrosyl complexes, it likely comes from the successive formation of different nitrite complexes at increasing nitrite concentrations. In order to assign this peak split to specific ruthenium complexes, DFT calculation have been performed to simulate RAMAN spectra of ruthenium complexes with a different number and position of nitrite ligands. It demonstrates that the ruthenium coordination involves a replacement of nitrate ligands in 1 mol/L as well as in 5 mol/L nitric acid. The replacement of nitrate ligands in 1 mol/L nitric acid preferentially forms ruthenium nitrosyl complexes with three nitrites in equatorial position and two water ligands. In 5 mol/L nitric acid, the replacement preferentially forms ruthenium nitrosyl complexes with two nitrites in cis position and at least one nitrate ligand remaining in the equatorial plane.

THE IMPACT OF NITRITE ON RUTHENIUM ORGANIC PHASE SPECIATION

Nitrous acid has an impact on a number of elements in solvent extraction cycles, such as neptunium. In the previous section, we reported reactions between nitrous acid and ruthenium nitrosyl compounds. The results show that nitrites from nitrous acid can complex ruthenium, forming ruthenium(III) nitrosyl nitrite compounds. However, ruthenium extraction with TBP solvents or other extracting molecules have not been studied for aqueous solutions with different nitrous acid concentrations yet. Herein, we analysed the impact of nitrous acid on the extraction of ruthenium by TBP and TODGA. In Figure 6 we show that the addition of sodium nitrite changes the distribution ratio of ruthenium at different nitric acid concentrations in solvent extraction experiment.

This project has received funding from the EURATOM research and training programme 2014–2018 under grant agreement No 730227

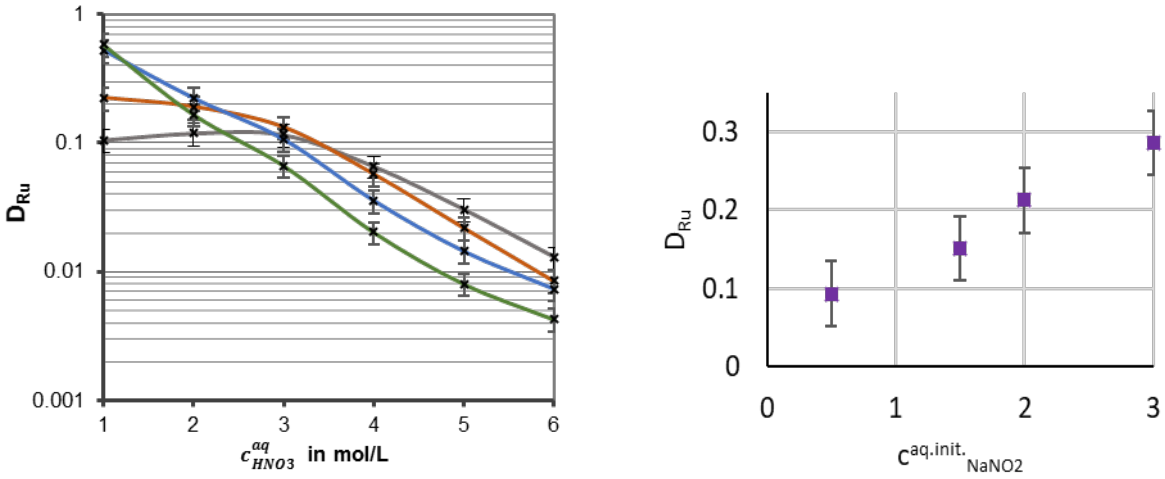

Figure 14. Left, ruthenium distribution ratios for extraction with 1.1 mol/L TBP in TPH as a function of the initial nitric acid concentration. The aqueous solutions initially contained zero (gray), one (orange), two (blue) or three (green) equivalents of nitrite per ruthenium complex. Right, ruthenium distribution ratio for extraction with 0.1 mol/L TODGA in TPH as a function of the initial sodium nitrite concentration with constant 3 mol/L nitric acid concentration.

Both TBP and TODGA result shown strong modifications of the extracting properties in presence of nitrite ions. With TBP it increases the D_{Ru} for low nitric acid concentration whereas it slightly decreases it at higher HNO_3 concentrations. For the TODGA system only extraction at 1M nitric acid were studied, but it also shows the strong impact of nitrite ions on the ruthenium extraction properties.

To illustrate this effect, Figure 15 shows the corresponding FTIR spectra of TODGA contacted with ruthenium(III) nitrosyl nitrate in 1 mol/L nitric acid with different initial concentrations of sodium nitrite. For clarity the spectra were subtracted to the initially pre-equilibrated organic phase FTIR signal as for the extraction studies without nitrite (see section “Solvent extraction from nitric acid solution” above).

This project has received funding from the EURATOM research and training programme 2014–2018 under grant agreement No 730227

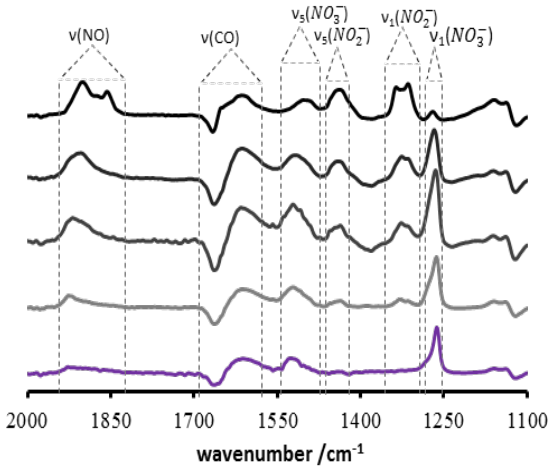

Figure 15. FTIR spectra of initially 0.6 mol/L ruthenium (III) nitrosyl nitrate solutions in 1 mol/L nitric acid extracted into 0.2 mol/L TODGA 5 $\%_{vol}$ 1-octanol in TPH. Aqueous phases initially contained (from top) 3 mol/L, 2 mol/L, 1.5 mol/L, 0.5 mol/L and 0 mol/L sodium nitrite. Table 1: corresponding vibration assignment.

Table 2. Assignment corresponding to Figure 15.

Assignment	wave number [cm^{-1}]	Description
v(NO)	1900	Nitrosyl stretching
v(CO)	1600	TODGA carbonyl stretching
$\nu_5(NO_3^-)$	1530	Nitrate stretching
$\nu_5(NO_2^-)$	1420	Nitrite stretching
$\nu_1(NO_3^-)$	1320	Nitrate stretching
$\nu_1(NO_2^-)$	1260	Nitrite stretching

As the ruthenium is extracted by the TODGA organic phase, a $\nu_{(NO)}$ signal corresponding to the nitrosyl ligand arise from the differential spectra (pre-equilibrated solvent signal subtracted). This signal provides two complementary information. It is indirectly related to the ruthenium distribution ratio and rise with amount of extracted ruthenium. Its position is modified depending on the five remaining ligands present in the ruthenium coordination sphere. Firstly, it is consistent with the D_{Ru} measured as a function the initial nitrite concentration (Figure 6). Secondly, the other FTIR signals corresponding to nitrite and nitrate ligand in the ruthenium coordination sphere as well as the carbonyl vibration also indicate changes in the organic ruthenium speciation.

The carbonyl stretching frequencies changes as the TODGA modified its interaction within the organic phase species. As the ruthenium is extracted, two medication can be noted:

- A negative value at 1650 cm^{-1} (again relative the pre-equilibrated organic phase) indicates the decrease in TOGDA-HNO_3 interactions

This project has received funding from the EURATOM research and training programme 2014–2018 under grant agreement No 730227

- The positive signal is presumably due to an inner sphere TODGA interaction with Ruthenium complexes

The nitrite signals at about 1420 and 1320 cm^{-1} for the symmetric and asymmetric stretching frequencies respectively arise as expected with the ruthenium concentration in the organic phase as well as with the number of nitrite ligand in ruthenium complexes coordination sphere. The split of the $\nu_1(NO_2)$ band related to different Ru nitrite complexes/stoichiometry further evidences this effect. As the nitrite, ligands feel the ruthenium coordination sphere, from mononitrite to (cis) dinitirite and finally trinitrite, the nitrite stretching frequencies is modified and two peaks arise. Such a split and change in shape was confirmed by DFT calculation on ruthenium complexes with various nitrite ligand configuration.

Concomitantly the nitrate ligand peaks $\nu_5(NO_3)$ and $\nu_1(NO_3)$ are also proportional to D_{Ru} with an increase in intensity. The competition of nitrite and nitrate in the ruthenium coordination sphere results in a strong suppression of the nitrate signal for higher nitrite concentrations.

Overall, it is clear that nitrite complexes differ distinctly from nitrate complexes in solvent extraction experiments. As the ruthenium complex's structure is modified in both aqueous and organic solutions, the resulting extraction properties change. In contrast to all previous experiments performed in absence of significant nitrite concentrations, there is also evidences for the extracting molecule entering the ruthenium nitrite complex first coordination sphere. Certainly, this change in coordination mode may affect the overall ruthenium extraction properties and may help to understand some of the retention mechanisms described in the following section.

RETENTION MECHANISM

REVEALING RETENTION MECHANISM IN RUTHENIUM SOLVENT EXTRACTIONS

In current PUREX processes, ruthenium is known for its unusual behaviour in solvent extraction scrubbing cycles. Once ruthenium nitrosyl complexes are extracted into the TBP organic phase, they are notably hard to remove in scrubbing stages at low nitric acid concentrations. Figure 16 shows ruthenium distribution ratio as a function of the initial nitric acid concentration in aqueous solution for (a) TODGA, (b) MOEHA and (c) TBP. The black point and coloured line are the distribution ratio under extraction conditions (ruthenium initially in the aqueous phase) equivalent to Figure 10. The red cross and diamond assigned with A and B on Figure 16 correspond to distribution ratio obtained under the low acidic and high acidic scrubbing conditions (ruthenium is first extracted to organic solution from a 3M nitric acid solution and then back extracted by 2 mol/L nitric acid solution and 3 mol/L nitric acid solution). The two acidic conditions for this experiment were selected to represent (i) the first

This project has received funding from the EURATOM research and training programme 2014–2018 under grant agreement No 730227

stripping step in solvent extraction systems industrially applied with TBP (2 mol/L) and (ii) to check consistency in distribution ratio between extraction and striping (3 mol/L) — indeed verified for the three systems since A points are in the extraction isotherms.

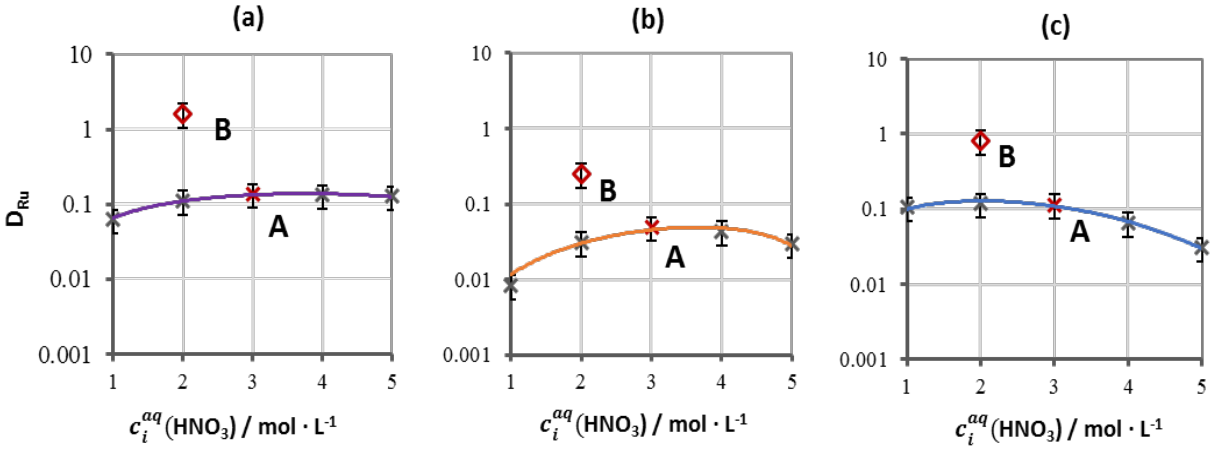

Figure 16. Distribution ratios of ruthenium as a function of the nitric acid concentration for extraction into (a) 0.2 mol/L + 5 $\%_{vol}$ 1-octanol in TPH, (b) 1.4 mol/L MOEHA in TPH and (c) 1.1 mol/L TBP in TPH. The point A and B represent extraction and scrubbing conditions, respectively, as in the PUREX process.

As already mentioned, the curves show that TODGA (a) and MOEHA (b) globally extract ruthenium in the same order of magnitude as TBP (c) and with distribution ratios below 1. This promotes using such solvents to separate ruthenium from uranium. Nevertheless, in face of TBP, ruthenium extractions with TODGA and MOEHA differs both at low and at high nitric acid concentrations as observed with the different bell-shaped curves. At high nitric acid concentrations (4 and 5 mol/L), ruthenium distribution ratios are similar to those at 3 mol/L, suggesting a secondary extraction process not competing with nitric acid extraction. Ruthenium extraction by MOEHA at low nitric acid concentration exhibit the lowest ruthenium distribution ratios. This was explained previously reporting the formation of the hydrolysed ruthenium complex extracted below c^{aq}_{HNO3} = 3 mol/L. This complex is only observed with TODGA and TBP but is never formed in the case of MOEHA.

Considering now the scrubbing experiment, a potential retention process is highlighted in all three cases. In the successive extraction and scrubbing experiment (red marks), all extractants show point B above the extraction isotherm (low acidic scrubbing). This reveals the retention effect. Retention means that back extraction from the organic into an aqueous phase shows higher ruthenium distribution ratios than the corresponding extraction at the same nitric acid concentration. Accordingly, the retention behaviour of ruthenium similarly appears in different solvent extraction systems with oxygen-donor molecules.

This project has received funding from the EURATOM research and training programme 2014–2018 under grant agreement No 730227

SPECULATIVE DISCUSSION ON THE ORIGIN OF RUTHENIUM RETENTION

Currently there is no fully adequate explanation for the retention phenomenon of ruthenium. The difference in distribution ratio between extraction and back extraction is independent of the extraction system and hence might concern the ruthenium coordination sphere itself. Speciation study identified numerous transformations of ruthenium in solvent extraction cycles that could explain the retention phenomenon. For instance, enlarged nitrous acid concentration in the initial aqueous phase strongly changes extracted species of ruthenium and could be involved in the retention process. In this case, the change in coordination mode of the extracting molecule may be involved in this process (inner sphere vs. outer sphere coordination). The impact of hydroxide ligand in the striping steps must be considered too since. Moreover, future studies to understand and predict the retention mechanism likely deserve kinetic experiments since ruthenium nitrosyl complexes are known slowly exchanges ligands.

CONCLUSION

Overall, the ruthenium extraction and back extraction was studied for different extraction systems all showing promising properties in means of ruthenium selectivity (low D_{Ru}). Nevertheless, the retention mechanism identified already for TBP is also evidenced for the other studied extracting molecule (TODGA, MOEHA). From the speciation analysis, we described the similarity in the ruthenium extraction process for the three studied systems mostly involving a weak hydrogen bond base ruthenium-ligand interaction. Without nitrite ions and under 3–4 mol/L nitric acid conditions, the ruthenium is extracted as nitrosyl trinitrate di aquo complexes hydrogen bonded through the water ligand to the extracting molecule. Consequently, we demonstrated that, in first approximation, the ruthenium extraction properties of a given solvent are strongly related to its ability to extract water.

Further experiments demonstrated that nitrite (so far neglected) is also important for this system because it strongly interacts with ruthenium complexes in both aqueous and organic phases. Nitrite ions are stabilised for several weeks in the ruthenium coordination sphere even under highly acidic conditions. This effect appears to modify the ruthenium distribution ratio and seems important for the right prediction of Ru extraction properties. Moreover, the great change in the extracting molecule coordination mode (outer to inner sphere) in presence of nitrite ligands seems important to anticipate the molecular interaction in the organic phase.

This nitrite effect is one clue to explain the ruthenium retention mechanism that was evidenced in the last part of this work. But, as already mentioned, there is still no fully satisfying explanation to explain the variation observed for D_{Ru} in the stripping steps and further kinetic studies should help to solve this puzzle.

This project has received funding from the EURATOM research and training programme 2014–2018 under grant agreement No 730227

REFERENCES

1. Sasaki, Y.; Sugo, Y.; Suzuki, S.; Tachimori, S., The novel extractants, diglycolamides, for the extraction of lanthanides and actinides in HNO3/n-dodecane system. *Solvent Extr. Ion Exch.* **2001,** *19* (1), 91–103.

2. Modolo, G.; Asp, H.; Schreinemachers, C.; Vijgen, H., Development of a TODGA based process for partitioning of actinides from a PUREX raffinate part I: batch extraction optimization studies and stability tests. *Solvent Extr. Ion Exch.* **2007,** *25* (6), 703–721.

3. Ansari, S. A.; Pathak, P.; Mohapatra, P. K.; Manchanda, V. K., Chemistry of diglycolamides: promising extractants for actinide partitioning. *Chem. Rev.* **2012,** *112* (3), 1751–1772.

4. Whittaker, D.; Geist, A.; Modolo, G.; Taylor, R.; Sarsfield, M.; Wilden, A., Applications of diglycolamide based solvent extraction processes in spent nuclear fuel reprocessing, part 1: TODGA. *Solvent Extr. Ion Exch.* **2018,** *36* (3), 223–256.

5. Modolo, G.; Geist, A.; Miguirditchian, M., Minor actinide separations in the reprocessing of spent nuclear fuels: recent advances in Europe. In *Reprocessing and Recycling of Spent Nuclear Fuel*, Taylor, R., Ed. Woodhead Publishing: Cambridge, UK, 2015.

6. Weßling, P.; Müllich, U.; Guerinoni, E.; Geist, A.; Panak, P. J., Application of aromatic TODGA solvents for An(III) and Ln(III) extraction requiring no modifier to suppress third phase formation. *Hydrometallurgy* **2019,** *(submitted)*.

7. Wilden, A.; Modolo, G.; Kaufholz, P.; Sadowski, F.; Lange, S.; Sypula, M.; Magnusson, D.; Müllich, U.; Geist, A.; Bosbach, D., Laboratory-scale counter-current centrifugal contactor demonstration of an innovative-SANEX process using a water soluble BTP. *Solvent Extr. Ion Exch.* **2015,** *33* (2), 91–108.

8. Wagner, C.; Müllich, U.; Geist, A.; Panak, P. J., Selective extraction of Am(III) from PUREX raffinate: the AmSel system. *Solvent Extr. Ion Exch.* **2016,** *34* (2), 103–113.

9. Lefebvre, C.; Dumas, T.; Tamain, C.; Ducres, T.; Solari, P. L.; Charbonnel, M.-C., Addressing ruthenium speciation in tri-n-butyl-phosphate solvent extraction process by fourier transform infrared, extended X-ray absorption fine structure, and single crystal X-ray diffraction. *Ind. Eng. Chem. Res.* **2017,** *56* (39), 11292–11301.

10. Boswell, G. G. J.; Soentono, S., Ruthenium nitrosyl complexes in nitric acid solutions. *J. Inorg. Nucl. Chem.* **1981,** *43* (7), 1625–1632.

11. Lefebvre, C.; Dumas, T.; Charbonnel, M. C.; Solari, P. L., Speciation of ruthenium in organic TBP/TPH organic phases: a study about acidity of nitric solutions. *Proc. Chem.* **2016,** *21*, 54–60.

12. Siczek, A. A.; Steindler, M. J., *Atomic Energy Review* **1978,** *16*, 575–618.

13. Lefebvre, C., Spéciation du ruthénium dans les phases organique TBP/TPH (structure et réactivité). **2018**.

14. Dirks, T.; Dumas, T.; Solari, P. L.; Charbonnel, M.-C., Ruthenium nitrosyl structure in solvent extraction systems: a comparison of tributyl phosphate, tetrabutyl urea, N-methyl, N-octyl ethylhexanamide, and N,N,N',N'-tetraoctyl diglycolamide. *Ind. Eng. Chem. Res.* **2019,** *58* (32), 14938–14946.

15. Fletcher, J. M.; Lyon, C. E.; Wain, A. G., The partition coefficients of nitratonitrosylruthenium complexes between nitric acid and TBP phases. *J. Inorg. Nucl. Chem.* **1965,** *27* (8), 1841–1851.

16. Il'yin, M. A.; Emel'anov, V. A.; Belyaev, A. V.; Makhinya, A. N.; Tkachev, S. V.; Alferova, N. I., New method for the synthesis of trans-hydroxotetraamminenitrosoruthenium(II) dichloride and its characterization. *Russian Journal of Inorganic Chemistry* **2008,** *53*, 1070–1076.

This project has received funding from the EURATOM research and training programme 2014–2018 under grant agreement No 730227

17. Kabin, E. V.; Emel'yanov, V. A.; Vorob'yev, V. A.; Alferova, N. I.; Tkachev, S. V.; Baidina, I. A., Reaction of trans-[RuNO(NH3)4(OH)]Cl2 with nitric acid and synthesis of ammine (nitrato) nitrosoruthenium complexes. *Russian Journal of Inorganic Chemistry* **2012,** *57*, 1146–1153.

18. Ferraro, J. R., The nitrate symmetry in metallic nitrates. *Journal of Molecular Spectroscopy* **1960,** *4* (2), 99–105.

19. Moeyaert, P.; Dumas, T.; Guillaumont, D.; Kvashnina, K.; Sorel, C.; Miguirditchian, M.; Moisy, P.; Dufrêche, J.-F., Modeling and speciation study of uranium(VI) and technetium(VII) coextraction with DEHiBA. *Inorg. Chem.* **2016,** *55* (13), 6511–6519.

This project has received funding from the EURATOM research and training programme 2014–2018 under grant agreement No 730227